DOI: 10.1590/2317-4889201820170072

ARTICLE

Processing of large offset data: experimental seismic line from Tenerife Field, Colombia

Francisco Gamboa Ortega[1], Amin Bassrei[1]*, Ellen de Nazaré Souza Gomes[2], Michelângelo Gomes da Silva[1], Andrei Gomes de Oliveira[2]

ABSTRACT: *Exploration seismology provides the main source of information about the Earth's subsurface, which in many cases can be presented as a simple model of horizontal or near-horizontal layers. After the seismic acquisition step, conventional seismic processing of reflection data provides an image of the subsurface by using information about the reflections of these layers. The traveltime from a source to different receivers is adjusted using a hyperbolic function. This expression is used in the case involving an isotropic medium, which is a simplification of nature, whereas geologically complex media are generally anisotropic. A subsurface model that more closely resembles reality is the vertical transverse isotropy, which defines two parameters that are required to correct the traveltimes: the NMO velocity and the anellipticity parameter. In this paper, we reviewed the literature and methodology for velocity analysis of seismic data acquired from anisotropic media. A model with horizontal layers and anisotropic behavior was developed and evaluated. The anisotropic velocity was compared to the isotropic velocity, and the results were analyzed. Finally, the methodology was applied to real seismic data, i.e. an experimental landline from Tenerife Field, Colombia. The results show the importance of the anellipticity parameter in models with anisotropic layers.*

KEYWORDS: *non-hyperbolic velocity analysis; anisotropy; anellipticity parameter; experimental seismic line.*

INTRODUCTION

The main objective of exploration seismology is to obtain subsurface images that may indicate possible hydrocarbon reservoirs after proper interpretation. In the seismic interpretation step, the images obtained from seismic reflection data should be faithful to subsurface characteristics. However, the seismic interpretation of geologically-complex media images is usually complicated. One factor that contributes to this difficulty is the type of processing performed on data. In many situations, the geological medium is not isotropic but anisotropic, that is, a given physical property varies with the direction. Accurate modeling of anisotropy features is frequently ignored in seismic data processing, especially since geologically-complex media in the quasi-static regime behave similarly to anisotropic media (Helbig 1994).

Several research studies demonstrated that the presence of a simple seismic anisotropy in a model, such as the vertical transverse isotropy (VTI) model, produces significant distortions in conventional seismic data analysis. For instance, the normal moveout (NMO) velocity is not equal to the root mean square (RMS) velocity, both for small and large offsets.

This type of medium produces a non-hyperbolic traveltime curve, which is manifested by significantly large offsets for PP-waves, i.e. a P-wave reflected as a P-wave. As to the PS-wave, i.e. a P-wave that converts to an S-wave in the reflection, this behavior is observed in both small and large offsets (Alkhalifah 1997). A possible solution would be to remove overcorrected traces and to stack all the others. Herein, the images could not provide the complete information.

In an anisotropic medium, the mathematical representation of the source-reflector-receiver traveltime can be expressed by a shifted hyperbola (Castle 1994). Such hyperbola

[1]Instituto de Geociências & Instituto Nacional de Ciência e Tecnologia de Geofísica de Petróleo, Universidade Federal da Bahia, Salvador (BA), Brazil. *E-mails: franciscogamboa12@gmail.com, bassrei@ufba.br, mgs@cpgg.ufba.br*

[2]Faculdade de Geofísica, Universidade Federal do Pará, Belém (PA), Brazil. *E-mails: ellensgufpa@gmail.com, andrei.jval@gmail.com*

*Corresponding author

Manuscript ID: 20170072. **Received on:** 05/21/2017. **Approved on:** 11/13/2017.

may be used to do the NMO correction with knowledge of three parameters:

- the zero offset source-reflector-receiver traveltime t_0;
- the NMO velocity V_{nmo};
- time-weighted moment of the velocity distribution (μ).

Alkhalifah and Tsvankin (1995) showed that three parameters are necessary for VTI media to perform the time processing:

- the zero offset source-reflector-receiver traveltime t_0;
- the NMO velocity V_{nmo};
- the anisotropy parameter η.

Fomel (2004) and Aleixo and Schleicher (2010) extended this parameterization by determining an approximation that was closer to exact data.

The objective of this paper was not to show the accuracy of the traveltime approximations found in literature, but to compare the NMO correction in synthetic and real data by using two techniques: one that depends on the NMO velocity estimate in addition to the anelasticity parameter η, and another that uses only the NMO velocity. The two techniques are based on the classical equations of Alkhalifah and Tsvankin (1995), and of Castle (1994) for the NMO correction Δt_{nmo}. Castle (1994) equation has the characteristic of using a displacement factor *S*, which may or may not depend on the anisotropy parameter η. When this parameter depends on η, the equation of Ursin and Stovas (2006) was implemented. The efficiency of these approaches was tested in a synthetic experiment with a five-layer model.

This article is organized as follows. First, the description of the two methods developed by Alkalifah and Tsvankin (1995) and Castle (1994), which corrects traveltime curves in anisotropic media, is reviewed. Then, these two methodologies are applied to synthetic data and real data acquired in the Tenerife Field, Magdalena Valley, Colombia. The experimental 2D seismic line is 9 km in length and presents large offsets of up to 5 km.

The methodologies (Alkalifah and Tsvankin 1995, Castle 1994) were validated by applying each method to synthetic and real data. The results show that the use of conventional seismic processing techniques for isotropic media may result in inconsistent results.

TRAVELTIME CALCULATION BY ALKHALIFAH AND TSVANKIN'S METHOD

The conventional velocity analyses methods typically used for seismic data processing assume an ideal reflector, i.e. a homogeneous reflector with flat interfaces and constant thickness. The medium is ideal, without energy loss and is also considered non-dispersive. The mathematical representation of the traveltime from the source to the receiver in a single-layer model is given by Equation 1:

$$t_x^2 = t_0^2 + \frac{x^2}{V_{nmo}^2} \quad (1)$$

Where:
x is the offset;
t_0 is the traveltime for zero offset;
t_x is the traveltime at the offset x; and
V_{nmo} is the NMO velocity. In conventional velocity analysis, the NMO velocity is denoted as the RMS velocity.

In a model with N flat layers, composed of an isotropic medium, the RMS velocity is calculated as Equation 2:

$$V_{rms}^2 = \frac{\sum_{i=1}^{N} v_i^2 t_i}{\sum_{i=1}^{N} t_i} \quad (2)$$

Where:
v_i is the interval velocity of the i-th layer and
t_i is the vertical traveltime of the i-th layer. The RMS velocity by Equation 2 refers to a set of N layers from the top of the first layer *(i = 1)* to the bottom of the last one *(i = N)*.

A more realistic representation of the traveltime equation implies knowledge of the anisotropic medium. For better results, with the appropriate resolution in the different events, it is important to take the medium's anisotropy into account.

For a medium with VTI anisotropy, the conventional method has several limitations, including the fact that the NMO velocity is not equal to the RMS velocity, whether in small or large offsets. An anisotropic medium produces a non-hyperbolic traveltime curve, which is more significantly manifested in large offsets in the case of PP waves. Regarding PS waves, this behavior is observed in all offsets, whether they are small or large (Alkalifah 1997).

To classify an offset by its size, we must consider the association between the offset x and the depth z. If $x/z>1.5$, the offset is considered large related to a non-hyperbolic traveltime curve. If this ratio is lower than 1.5, the offset will be small (Alkalifah 1997).

The standard NMO equation used by the industry only considers the first two terms of Taylor's series expansion,

which results in Equation 1. This treatment is suitable only for small offsets. For a VTI medium, we need to use more terms of the series to achieve an appropriate correction (Alkhalifah & Tsvankin 1995).

The Equation 3 adds a third term in Taylor's series expansion:

$$t_x^2 = t_0^2 + \frac{x^2}{V_{nmo}^2} - \frac{2\eta x^4}{V_{nmo}^2\left[t_0^2 V_{nmo}^2 + (1+2\eta)x^2\right]} \quad (3)$$

Equation 3 includes three unknowns: the zero offset traveltime t_0, the velocity V_{nmo}, and the new parameter η. Note that if η=0, Equation 3 is reduced to Equation 1.

The parameter η can be related to the well-known Thomsen's anisotropic parameters ε, δ and γ (Thomsen 1986). Parameters ε and δ satisfy the following conditions:

$$|\delta| << 1, \; |\varepsilon| << 1$$

in which both terms zero in an isotropic medium. The value of γ will be considered zero in this paper, because we are assuming a two-dimensional wave propagation in the zx plane. A fourth parameter, η, is defined as in Equation 4,

$$\eta = \frac{\varepsilon - \delta}{1+2\delta} \quad (4)$$

and represents the anisotropic approximation of anellipticity introduced by Alkhalifah and Tsvankin (1995). This parameter is called anellipticity, and it is usually positive because it is very often $\varepsilon > \delta$ in seismic data.

We can define three types of wavefronts with these parameters:

- isotropic medium with a circular wavefront, in which $\varepsilon=\delta=0$;
- medium with elliptical anisotropy, in which $\varepsilon=\delta$; and
- medium with non-elliptical anisotropy.

Equation 3 can be generalized for a case with multiple layers, with the condition that V_{nmo} is equivalent to RMS velocity (Equation 5):

$$V_{rms}^2 = V_{nmo}^2 = \frac{\sum_{i=1}^{n} v_{nmo}^2 t_i}{\sum_{i=1}^{n} t_i} \quad (5)$$

Where, as in Equation 6:

$$v_{nmo} = v_i\sqrt{1+2\delta_i} \quad (6)$$

where:

v_i is the interval velocity; and

δ is the i-th layer Thomsen's parameter. In a multi-layer with VTI anisotropy, the value of η in Equation 3 is denoted by η_{eff} and expressed as Equation 7 (Alkhalifah 1997):

$$\eta_{eff} = \frac{1}{8}\left\{\frac{\sum_{i=1}^{n} v_{nmo}^4 t_i\left[1+8\eta_i\right]}{V_{nmo}^4 \sum_{i=1}^{n} t_i} - 1\right\} \quad (7)$$

We made a simulation example that explores the behavior of traveltime when anisotropy is present. Figure 1 shows the traveltime computed by Equation 3 as a function of the offset from a horizontal reflector at a depth of 1.582 km with V_{nmo}=3.893 (km/s) and η=0.026. The reflection before the NMO correction is shown in light blue circles. The traveltime curve, after NMO correction, is in blue using the correct value of η=0.026. The curve in black represents the wrong value of η=0.5 and the curve in red represents the value of η=0. Notice that, for example, η_{eff} is equal to η above because there is only one layer.

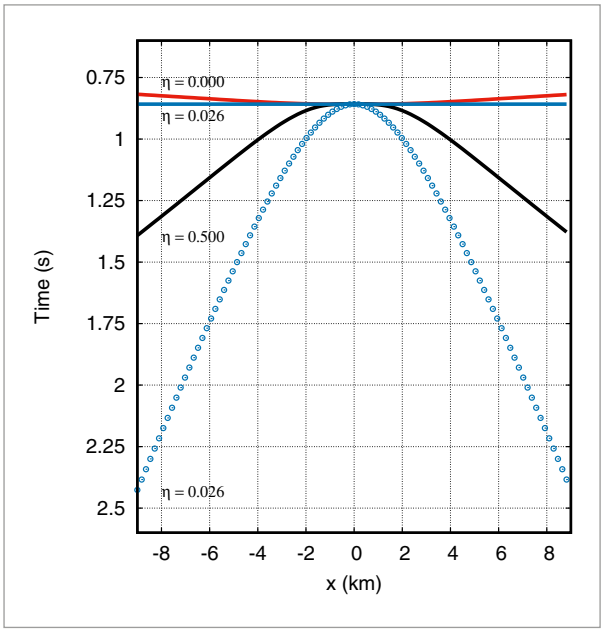

Figure 1. Reflection time as a function of the offset from a horizontal reflector at a depth of 1.582 km with V_{nmo}=3.893 km/s and η=0.026. The reflection prior to the NMO correction is shown in light blue circles. The reflection time curve after the NMO correction is presented in blue using the correct value of η=0.026. The curve in black represents the wrong value of η=0.5, and the curve in red represents the value of η=0.

Assuming a constant value of ε=0.2 and varying δ in the range from -0.2 to 0.2 in Equation 4, the values will fall within the range from 0.5 to 0. The value η=0 corresponds to the conventional or isotropic NMO correction. This NMO correction is accurate only for the condition $x/z \leq 1.5$ as shown in Figure 1. These data are from Thomsen (1986) and are specific to the Mesaverde sandstone.

TRAVELTIME CALCULATION THROUGH CASTLE'S METHOD

Castle (1994) proposed an approach that requires three parameters:

- zero-offset source-reflector-receiver traveltime t_0;
- NMO velocity (V_{nmo})
- weighted moment (μ).

Equation 1 describes a symmetric hyperbola with respect to the time axis, whose asymptotes intersect at the coordinate system origin(x=0, t=0). Figure 2 illustrates this geometry, in which the solid curve represents the actual time curve of a reflector and the dashed curve represents the time computed using Equation 3. Asymptotes of the Dix or NMO equations are represented by dashed straight curves.

A more exact mathematical expression for the NMO correction was provided by Malovichko (1978) and used by Castle (1994), as in Equation 8:

$$t = \tau_s + \sqrt{\tau_0^2 + \frac{x^2}{v^2}} \tag{8}$$

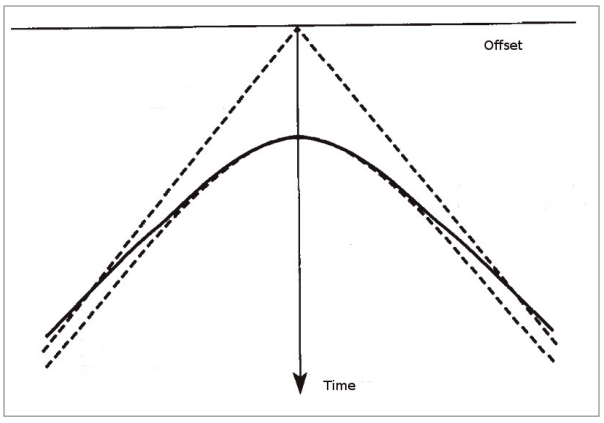

Figure 2. Geometry related to the Dix equation, in which the solid curve represents the real reflection time of a reflector, the dashed curve represents the time from the Dix equation (Dix 1955), and the dashed lines are asymptotes to the Dix equation (modified from Castle 1994).

where
τ_0 is expressed as Equation 9:

$$\tau_0 = \frac{t_0}{S} \tag{9}$$

and τ_s is the intersection time of the Dix equation hyperbola asymptotes with the time axis (Equation 10):

$$\tau_s = \tau_0 \left(S - 1\right) \tag{10}$$

In Equation 10, t_0 is the zero-offset double vertical time and v is an auxiliary variable expressed as Equation 11:

$$v^2 = SV_{rms}^2 \tag{11}$$

where the S factor is expressed as Equation 12:

$$S = \frac{\mu_4}{\mu_2^2} = \frac{\mu_4}{V_{rms}^4} \tag{12}$$

The value of μ_j, which is already called time-weighted moment of the velocity distribution, is expressed by Equation 13:

$$\mu_j = \frac{\sum \Delta\tau_k V_k^j}{\sum \Delta\tau_k} \tag{13}$$

where:
V_k is the interval velocity of the k-th layer; and
$\Delta\tau_k$ is the vertical time of the k-th layer.

Ursin and Stovas (2006) observed that the η factor introduced by Alkhalifah and Tsvankin (1995) and the S factor of the shifted hyperbola approximation are related by Equation 14:

$$S = 1 + 8\eta_{eff} \tag{14}$$

According to this relation, the displaced hyperbola approach can be used to describe the traveltime in VTI media.

Figure 3 illustrates the geometry of Equation 8, which describes shifted symmetric hyperbola (dashed curve) regarding the time axis, whose asymptotes intersect at point (x=0, t=τ_s). Figure 3 also shows the time curve of an actual reflector (solid curve) and the asymptotes of the shifted hyperbola equation (dashed straight curves). Comparing Figures 2 and 3, we observe that the NMO equation with a shifted offset hyperbola is a better approximation to data than the conventional Dix equation.

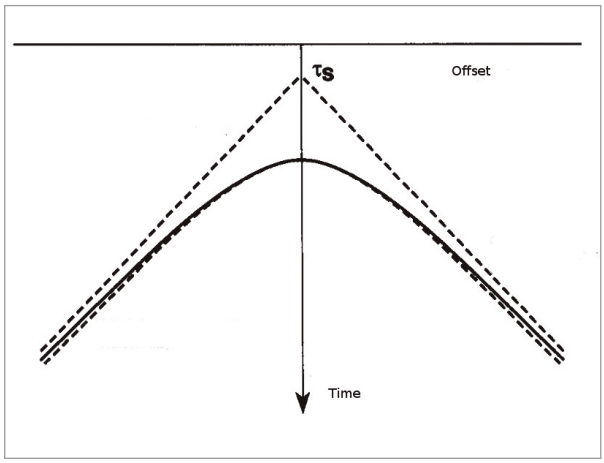

Figure 3. Geometry related to the shifted hyperbola equation, in which the solid curve represents the real reflection time of a reflector, the dashed curve represents the time from the Malovichko equation (1978), and the dashed lines are asymptotes to the shifted hyperbola equation. Notice that in relation to Figure 2, the two reflection times curves are much closer. Modified from Castle (1994).

SIMULATIONS WITH SYNTHETIC DATA

We used a five-layer model, shown in Figure 4, which has VTI-based anisotropy in the second, third, and fourth layers. Table 1 shows the elastic and anisotropic parameters. The offset depth ratio was greater than 1.5, with maximum offset of 9 km and maximum depth of 5 km. The parameters were chosen to be like the real data used in this work.

Figure 5 shows a Common Midpoint (CMP) with maximum fold, where four PP-wave reflections are easily identified and each reflection represents an interface. We also added noise in such a way that S/N =10. The ray tracing modeling was made with the seismic processing package SU – Seismic Unix (Stockwell Jr. 1997, Cohen & Stockwell 2010). Figure 6 shows the velocity analysis using the hyperbolic approximation for the CMP displayed in Figure 5, as well as the NMO-corrected CMP.

For large offsets in a VTI medium, we can use Equation 3 that has three unknown parameters: t_0, V_{nmo}, and η_{eff}. The search for these parameters can be separated into two steps. In the

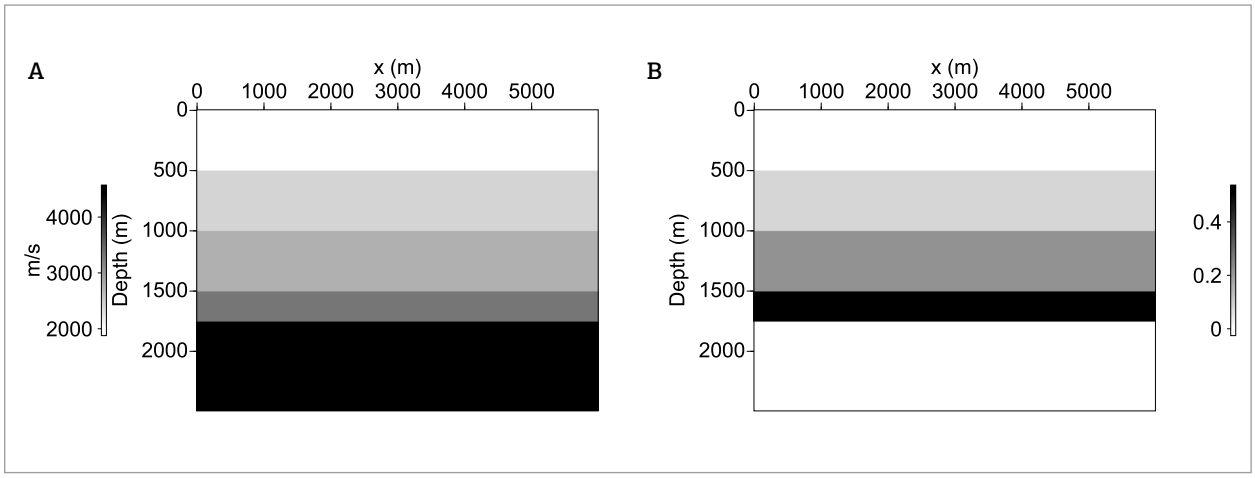

Figure 4. Layered model used to generate the synthetic seismogram: (A) P-wave vertical velocity; (B) anisotropic parameter. The first and last layers are isotropic, whereas the three intermediate layers are anisotropic. The parameters of each layer are shown in Table 1.

Table 1. Elastic and anisotropic parameters of the synthetic model.

Layer	$\rho(g/cm^3)$	ε	δ	η	$V_p(m/s)$	$V_s(m/s)$
1	2.16	0	0	0	2000	1400
2	2.23	0.081	-0.178	0.402	2409	1324
3	2.29	0.218	0.028	0.182	2757	1509
4	2.38	0.512	0.242	0.180	3308	2260
5	2.57	0	0	0	4450	2300

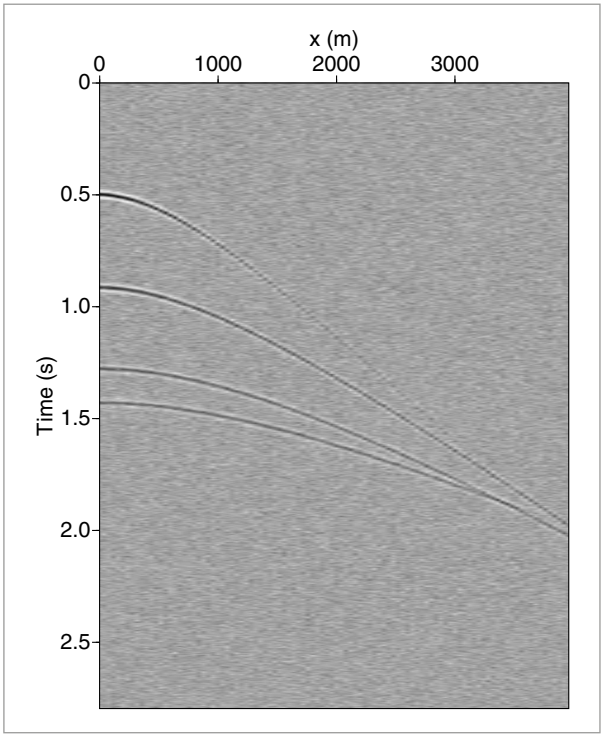

Figure 5. CMP gather for the model in Figure 4. The traveltimes were obtained using Seismic Unix (SU) ray tracing for a homogeneous anisotropic model.

first step, we need to obtain the t_0 and a velocity file from a conventional velocity analysis, which is still effective for relatively small offsets. In the second step, the velocities of the first step are used and they are kept constant. Subsequently, the value of η_{eff} is estimated by a coherence analysis, as shown in Figure 7A. We use the parameters obtained in the previous steps to apply the NMO correction through Equation 3, which provides an approximation for the traveltimes. This correction results in the horizontal curves observed in Figure 7B.

In the sequence, we applied Castle's (1994) method for NMO correction, which uses Malovichko's (1978) approach given by Equation 8. The velocity analysis (Figure 6A) provides the RMS velocity that is used in the Dix formula to obtain the interval velocity. Then, the interval velocity is used in Equation 13 for calculating the μ, which in its turn is used in Equation 12 to determine the value of parameter S. Finally, with the value of S, we obtain the seismic section of Figure 8A, in which we observe that for offsets above 2,000 m there is a significant difference between this result and the conventional NMO correction seen in Figure 6B. We also applied the NMO correction using Ursin and Stovas (2006) traveltime approximation, where two input data are necessary: the estimation of the RMS velocity, like the standard Castle's method, and the parameter η_{eff}, which is obtained from the coherence analysis

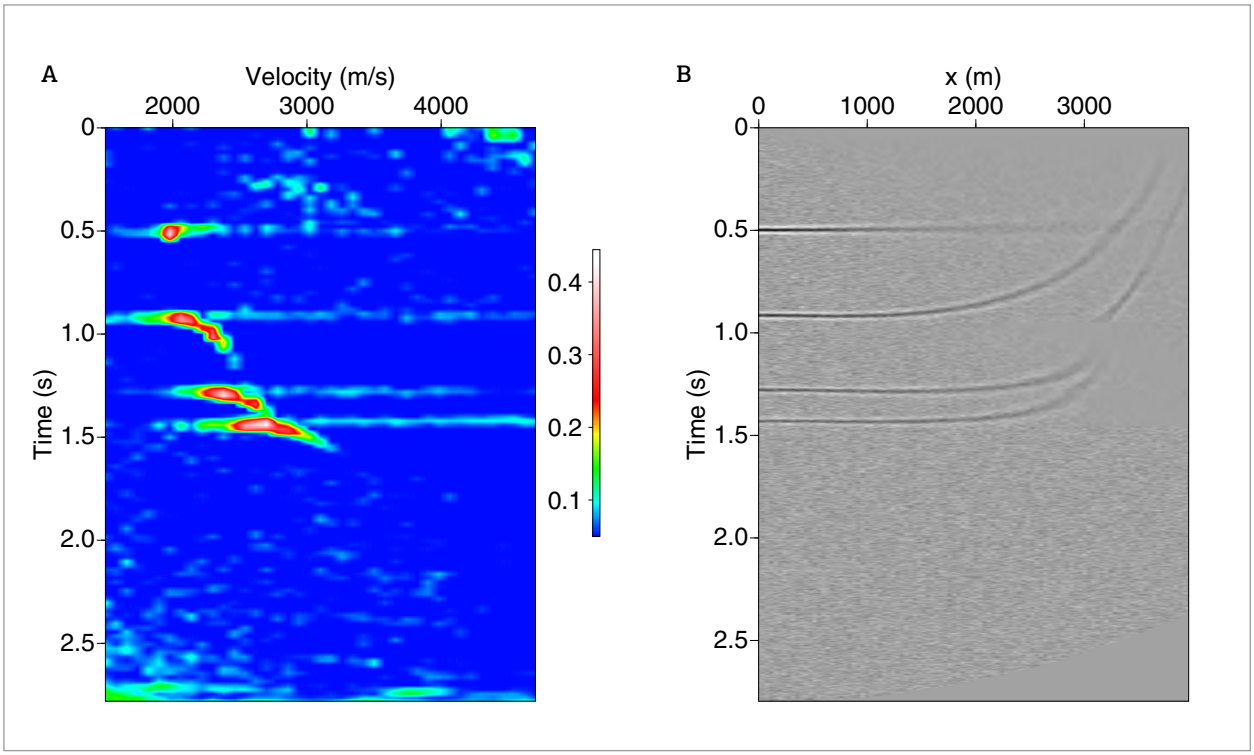

Figure 6. (A) Velocity spectra using SU in the CMP gather displayed in Figure 5. (B) same gather as in Figure 5 after the isotropic moveout correction.

(Figure 7A). The result using Ursin and Stovas (2006) equation is the seismic section shown in Figure 8B. Comparing Figures 8A and 8B, the Castle's method was slightly better. This is true mainly for the second interface.

We also applied migration to these synthetic data. The NMO correction, either by the estimation of η_{eff} or by the calculation of *S*, reduces the NMO stretching for large offsets. This process is performed in the time domain, but

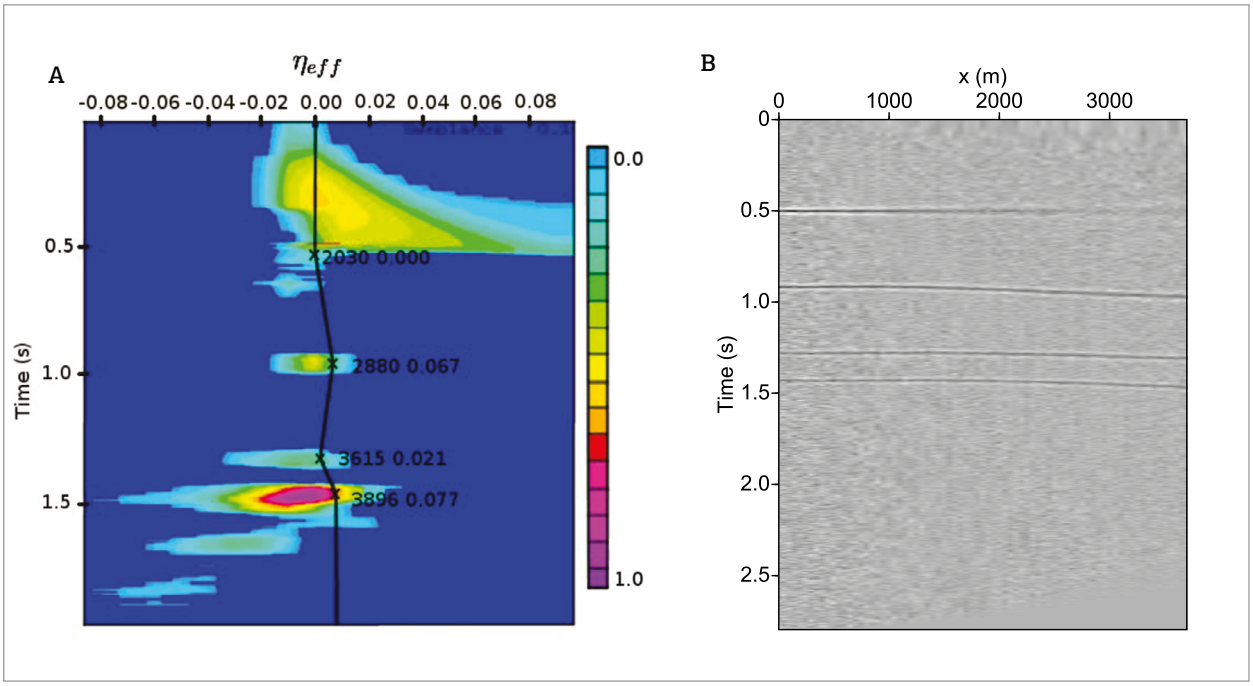

Figure 7. (A) Anisotropic parameter analysis using Focus of the CMP gather in Figure 5. (B) NMO-corrected CMP of the CMP gather in Figure 5 using the Alkhalifah and Tsvankin (1995) traveltime approximation.

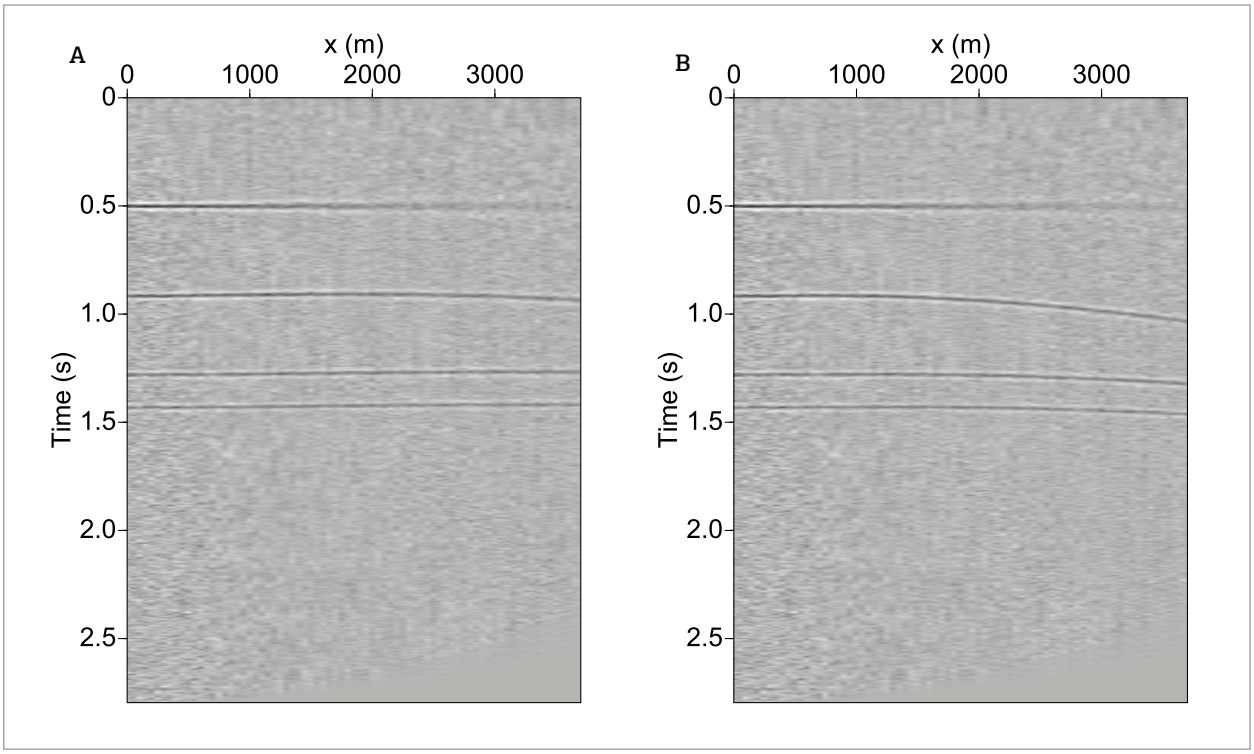

Figure 8. (A) NMO-corrected CMP of the CMP gather in Figure 5 using Castle (1994) traveltime approximation. (B) Same gather after moveout correction using the Ursin and Stovas (2006) traveltime approximation.

in an analogue way. In the depth domain, the phase-shift migration with anisotropic parameters implies in the collapse of diffractions associated with large offsets, even for a flat-layered model. The diffractions of the seismic section in Figure 9A, obtained after an isotropic pre-stack migration with 10 shots spaced 500 m apart using the model in Figure 4A, could be avoided in two ways:

- decreasing the distance between shots in the isotropic migration; or
- using an anisotropic migration, as shown in Figure 9B, in which we can see that the diffractions were collapsed.

In such case, the anisotropic migration was implemented for the same 10 shots spaced apart by 500 m. We used the depth-domain phase-shift migration with interpolation for both examples (Gazdag 1978, Gazdag & Squazzero 1984). For the isotropic case, the wavenumber in the depth direction is as seen in Equation 15:

$$k_z = \frac{\omega}{v}\sqrt{1-\frac{v^2 k_x^2}{\omega^2}} \tag{15}$$

and for the anisotropic case as in Equation 16 (Alkhalifah 2000):

$$k_z = \frac{V_{nmo}}{v}\sqrt{\frac{\omega^2}{V_{nmo}^2}-\frac{\omega^2 k_x^2}{\omega^2 - 2V_{nmo}^2 \eta k_x}} \tag{16}$$

where ω is the angular frequency, v is the vertical velocity of the medium, and k_x is the wavenumber in the x direction. For the migration experiments, the SU – Seismic Unix package was used.

The anisotropic migration was more effective than the isotropic. We can also observe the influence of large anisotropy parameters on the migration. For instance, in Figure 9A, the amount of noise in the second interface is a result of the large anisotropy parameters from the second layer.

To check the efficiency of the two methods used in this paper, we calculated the percentage error between the observed traveltimes and the times calculated by the approximation, using the estimator in Equation 17:

$$Error = \left|\frac{t_{obs} - t_{app}}{t_{obs}}\right| \times 100 \tag{17}$$

where t_{obs} is the observed traveltime and t_{app} is the traveltime computed by Equations 1, 3, and 8.

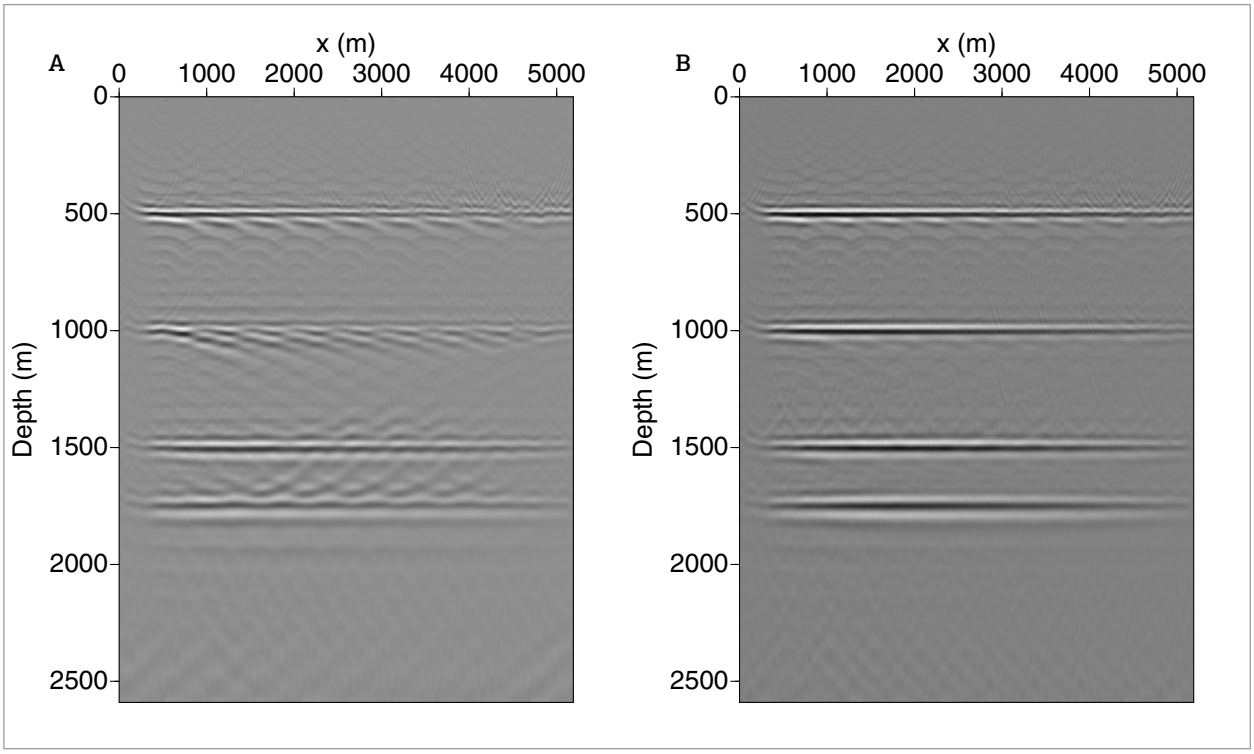

Figure 9. (A) Isotropic phase shift depth migration of the CMP stack using the P-wave vertical velocities from Figure 4A. (B) Anisotropic phase shift depth migration using the same true vertical velocities and the anisotropy parameter from Figure 4B.

For the multilayer model shown in Figure 4, a comparison between the presented approximations and the exact traveltimes from the interfaces is in Figure 10. We also computed the error given by Equation 17 for each interface. For the first interface, all approximations have the same behavior, that is, the errors were the same (see Figure 10A), because the first layer is isotropic. Alkhalifah and Tsvankin's (1995) approximation presents a smaller error than Castle's (1994) for the second and third interfaces, as seen in Figures 10B and 10C, respectively. The opposite occurs for the fourth interface, in which Castle's result is better.

The frequency distortion or NMO stretching observed for large offsets in Figure 6B can be expressed by Equations 18 and 19 (Yilmaz 1987):

$$\frac{\Delta f}{f} = \frac{\Delta t_{nmo}}{t_0} \tag{18}$$

$$\Delta t_{nmo} = t_{app} - t_0 \tag{19}$$

where: Δf is the frequency variation, f is the predominant frequency, and t_0 is the zero-offset traveltime. In conventional processing, the stretching effect is removed by muting a portion of the affected part.

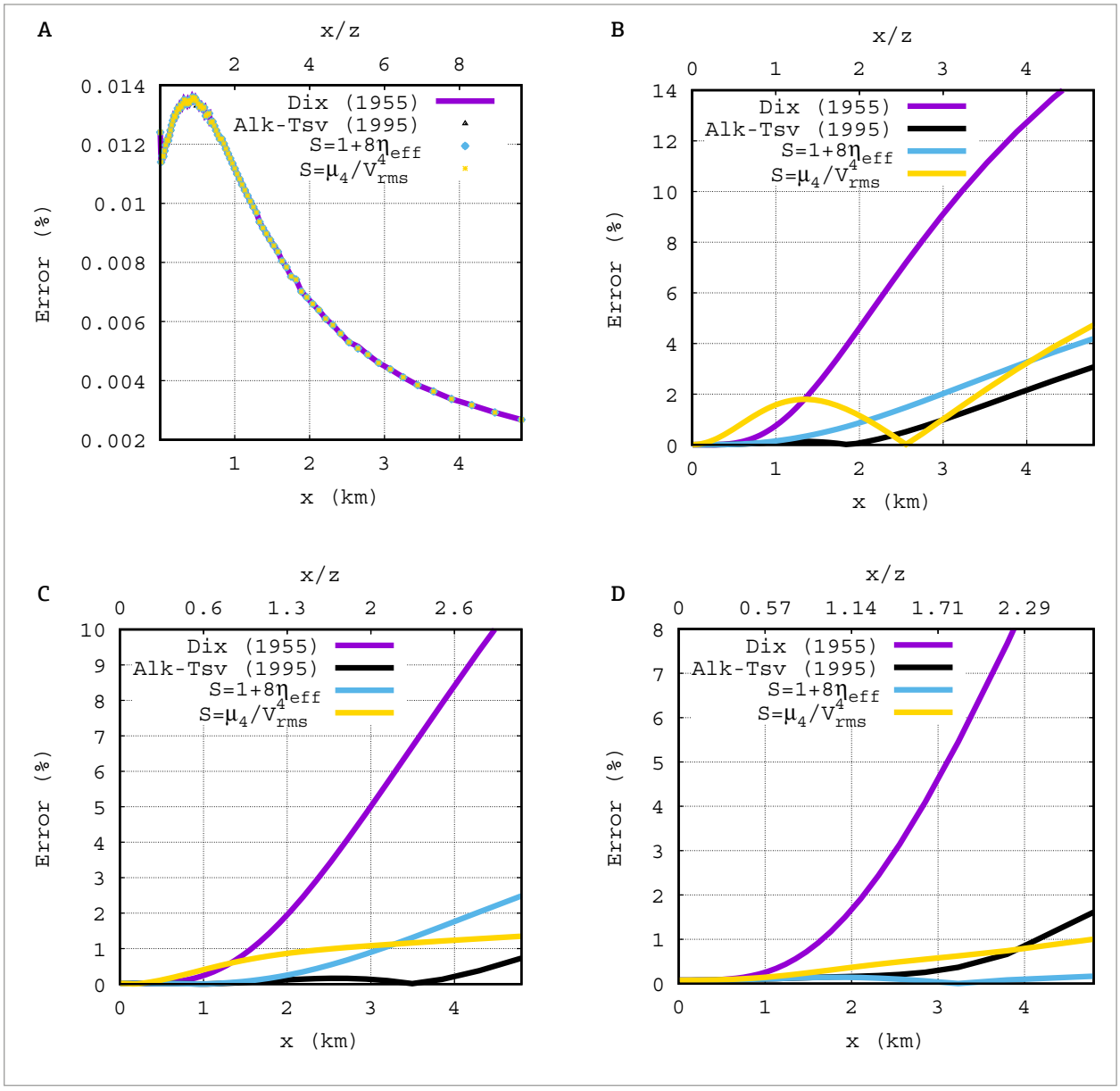

Figure 10. Relative error (%) of VTI traveltimes for the model displayed in Figure 4A comparing the approximations of Dix (1955), Alkhalifah and Tsvankin (1995) and Castle (1994) by using $S=1+8\eta_{eff}$ and Castle (1994) using $S=\mu 4/V^4_{rms}$: (A) first interface; (B) second interface; (C) third interface; (D) fourth interface.

The use of traveltime approximation equation, with more terms in the velocity analysis, improves the distortion problem, because the value of Δt_{nmo} decreases in Equation 18. This observation can be seen in Figures 7B, 8A and 8B; and no muting was applied in these figures.

In conclusion for this application, the compensation of anisotropy effects allows visualizing the reflector in all data, including large offsets. It is important to notice that in the conventional seismic data processing, sometimes the reflectors are edited and silenced, to not show the stretching effect.

APPLICATION TO REAL DATA

The proposed methodology was also used on real data to detect anisotropy. We used a 2D experimental land seismic line with maximum offset of 9,000 m, acquired in the Tenerife Field, Colombia. This field is in the Valle Médio del Magdalena Basin (VMMB), around 260 km distant from Bogota (Fig. 11). The basin is bordered to the North by the Bucaramanga Fault, inclined towards the East, with a homoclinal trend. It has an area of approximately 28,300 km^2, and the sediments can reach an 8,500 m thickness.

The Tenerife Field is represented by a polygon in Figure 12 and is structurally limited by a system of reverse faults. The seismic line, indicated by the green line in the same figure, was acquired in an area made up of 70% of mountainous terrain and 30% of plane ground. The elevation along the seismic line varied from 78 to 153 m. Three wells were drilled in the field (Tenerife 1, 2 and 3) reaching rocks from Tertiary and Cretaceous ages. There is oil production in the first two wells.

The real data (a 2D multi-component land seismic line) were from an exploration campaign conducted by Ecopetrol in 2010. Data were collected through continuous/sequential survey, using the Common Depth Point (CDP) technique

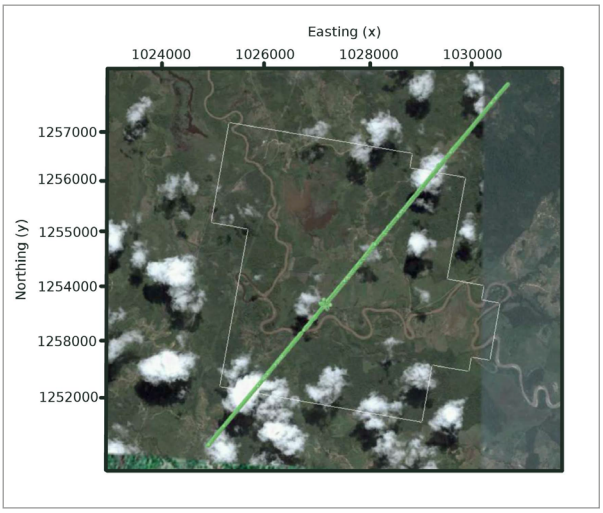

Figure 12. Satellite image showing the area of Tenerife Field and the location of the experimental seismic line (source: Ecopetrol).

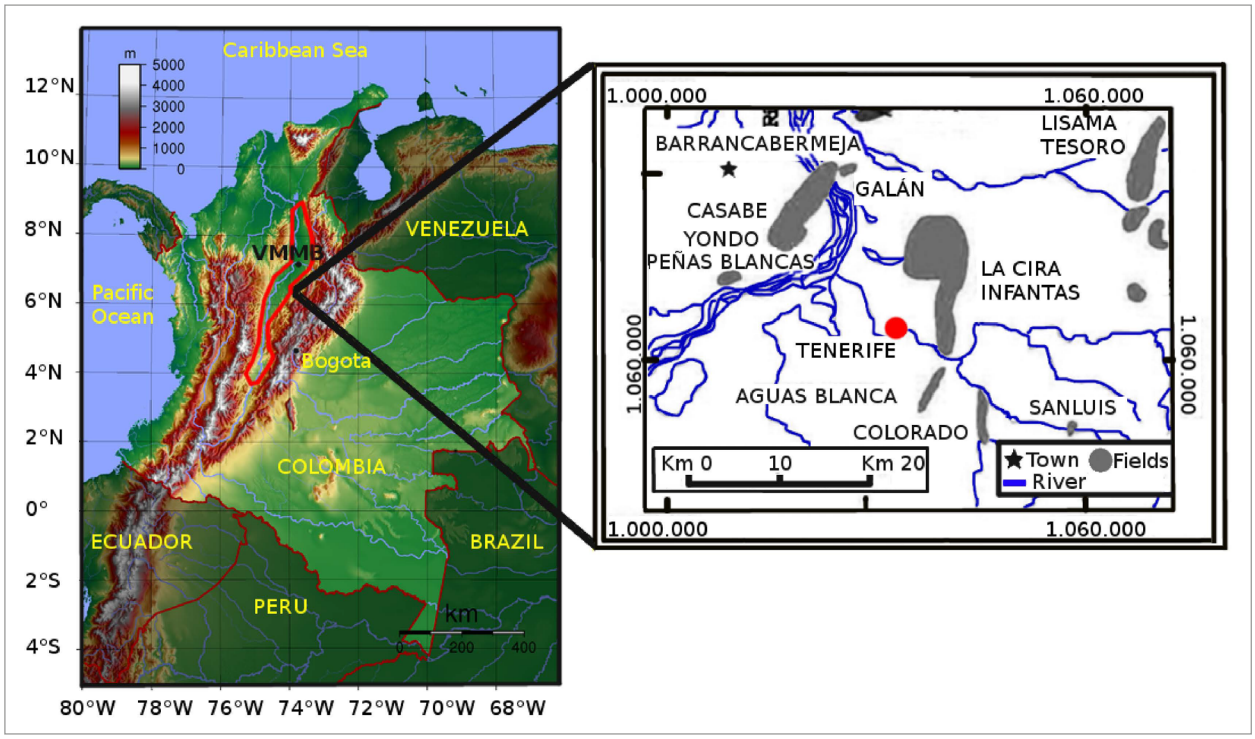

Figure 11. On the left, map showing the location of VMMB (Valle Médio del Magdalena Basin) in red, and on the right, the Tenerife Field (source: Google Maps and Ecopetrol).

and an asymmetrical array. The total length of the line was 9 km and there were 900 channels (accelerometers) per shot.

The same processing flow used for the synthetic data was applied to the Tenerife line. The results are in Figures 13, 14 and 15. Data were sorted in CDP families with maximum coverage, and the NMO correction was applied with zero stretch.

Figure 13 shows the result of conventional NMO correction using the Dix equation. One should pay attention to the stretching effects for offsets above 300 m from receivers 1 to 47. Figure 14 shows the result of NMO correction with Castle's method, and Figure 15 presents the result of NMO correction using Alkhalifah and Tsvankin's method with a constant η_{eff} equal to 0.1.

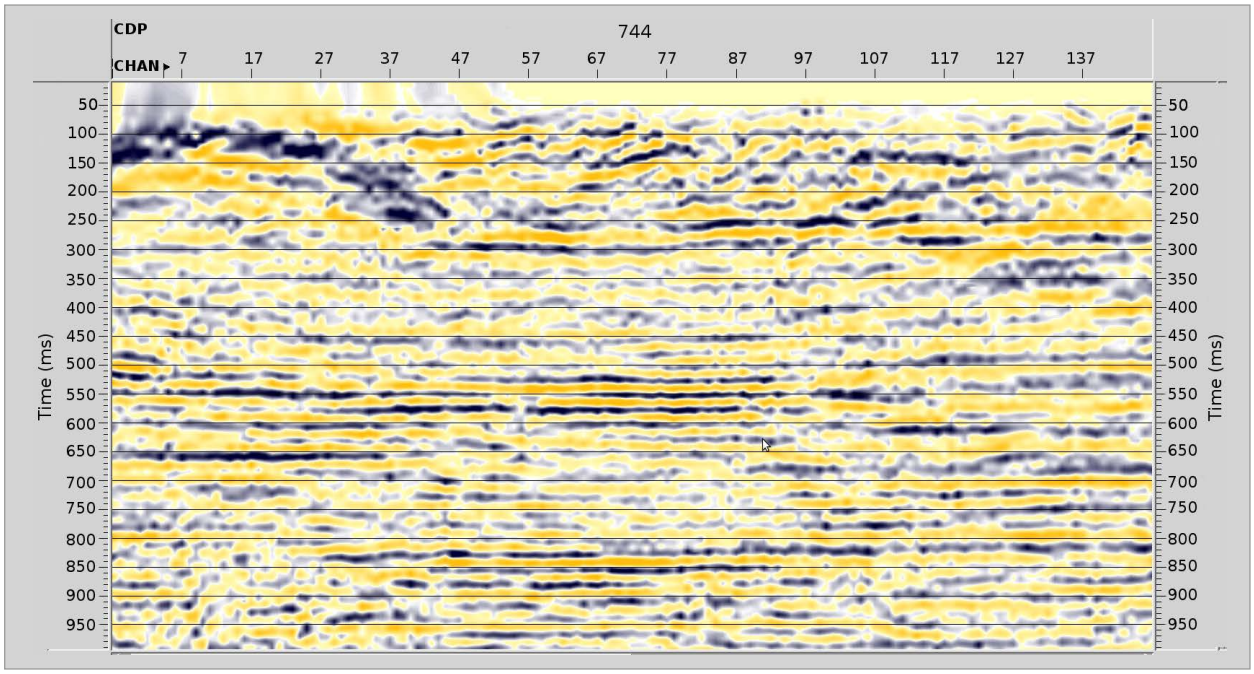

Figure 13. Seismic section using hyperbolic NMO correction with Dix (1955) equation.

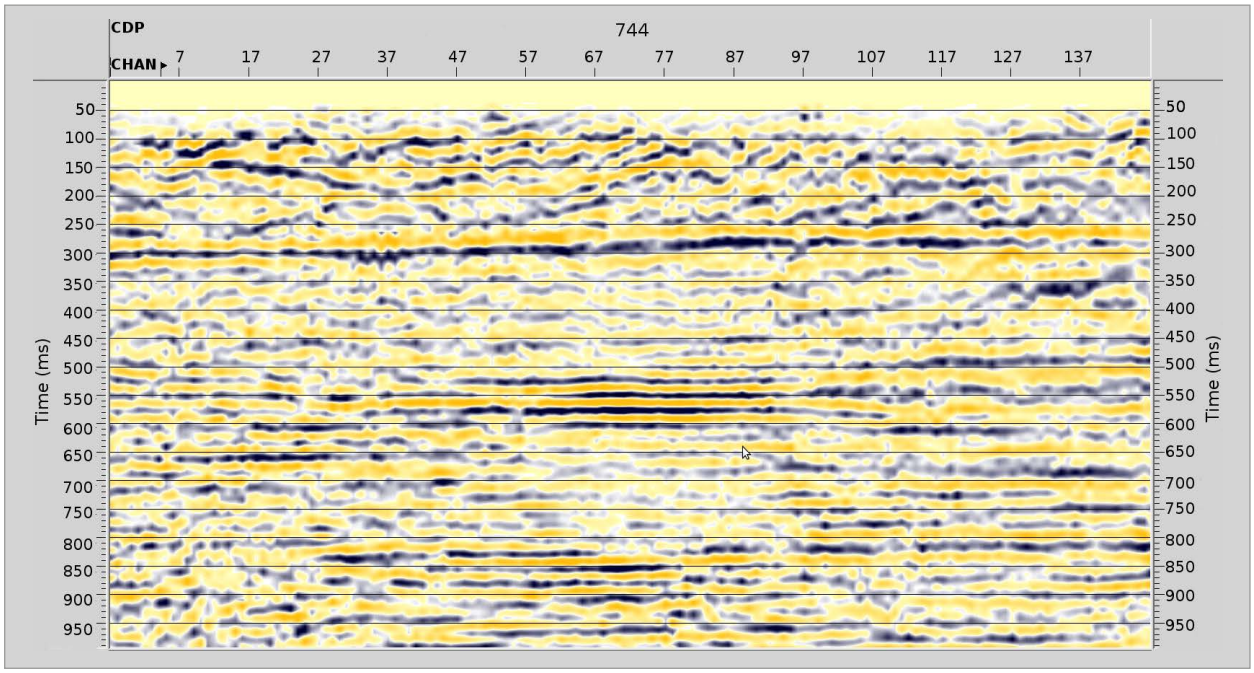

Figure 14. Seismic section using Castle (1994) NMO correction.

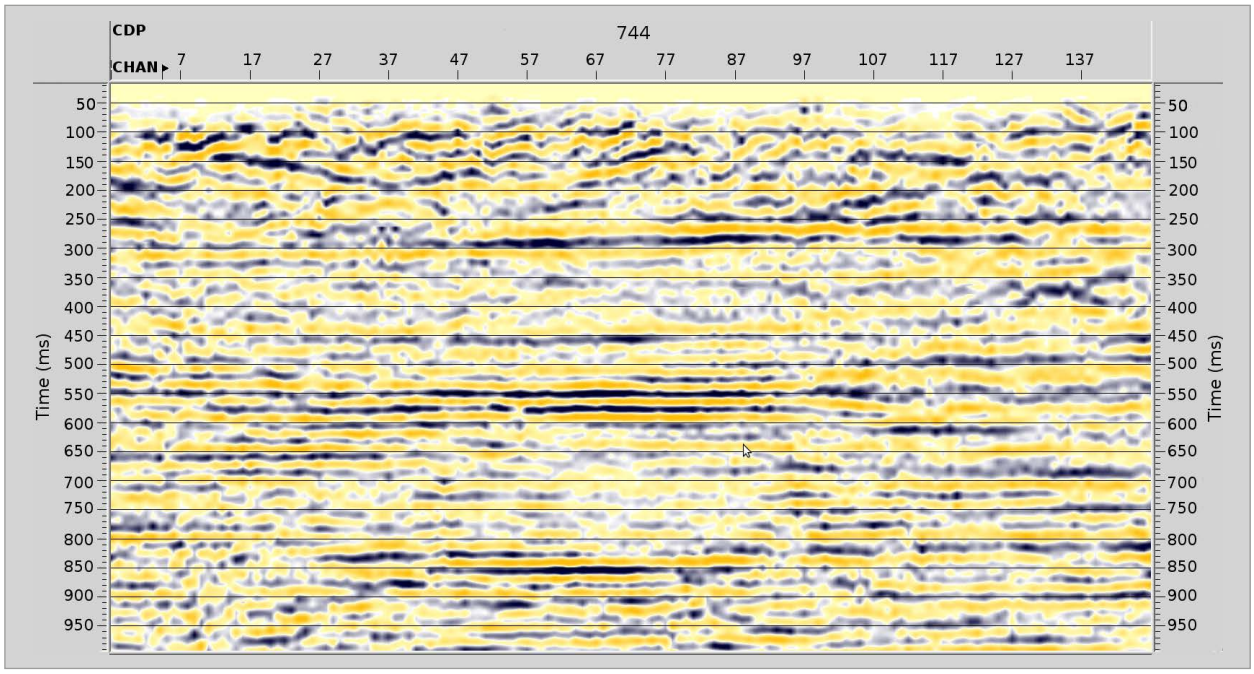

Figure 15. Seismic section using Alkhalifah and Tsvankin (1995) NMO correction with a constant value for η.

CONCLUSIONS

NMO correction produces distortions in frequency for shallow events as well as for large offsets. However, a portion of these distortions is removed in the conventional hyperbolic processing, thus deleting information from large offsets.

An anisotropic medium produces a non-hyperbolic reflection from a given interface, which is manifested more significantly for large offsets. Castle's method is a non-hyperbolic approach for NMO correction that does not depend on any anisotropy parameter but just a parameter *S,* which in turn depends on the interval time $\Delta\tau_k$ and interval velocity V_k of the k-th layer. A second non-hyperbolic approach was presented by Alkhalifah and Tsvankin, which makes use of an anisotropy parameter η_{eff}.

In this paper we applied the methods of Castle and Alkhalifah and Tsvankin for NMO correction, both in synthetic and real data. The real data were from an experimental seismic line from the Tenerife Field, Colombia. For the synthetic example, the simulations indicated that the relative traveltime error (between the observed traveltime and the traveltime provided by the approximation) was smaller for weak anisotropy, that is, for the third and fourth interfaces, when using Alkhalifah and Tsvankin's method. In addition, the error was also smaller for stronger anisotropy, i.e. for the second interface, when using Castle's method. The results indicate that NMO correction was successful, and in the case of real data, the images provided by Castle's method had a better quality for shallow events. On the other hand, the results using Alkhalifah and Tsvankin's equation on real data were consistent, despite the fact of keeping a constant value for η_{eff}. This suggests that a variable value for η_{eff} would improve the reflector imaging.

ACKNOWLEDGMENTS

F. Gamboa thanks *Coordenação de Aperfeiçoamento de Pessoal de Nível Superior* (CAPES) for receiving a scholarship. The authors thank Ecopetrol for the real data, *Conselho Nacional de Desenvolvimento Científico e Tecnológico* (CNPq), and PETROBRAS for supporting the project INCT – Petroleum Geophysics. We would also like to thank *Financiadora de Estudos e Projetos* (FINEP) for supporting the project Research Network in Geophysical Exploration, and Landmark and Paradigm for the academic software licenses.

REFERENCES

Aleixo R. & Schleicher J. 2010. Traveltime approximations for q-P waves in vertical transversely isotropy media. *Geophysical Prospecting*, **58**(2):191-201.

Alkhalifah T. & Tsvankin I. 1995. Velocity analysis for transversely isotropic media. *Geophysics*, **60**(5):1550-1566.

Alkhalifah T. 1997. Velocity analysis using nonhyperbolic moveout in transversely isotropic media. *Geophysics*, **62**(6):1839-1854.

Alkhalifah T. 2000. An acoustic wave equation for anisotropic media. *Geophysics*, **65**(4):1239-1250.

Castle R.J. 1994. A theory of normal moveout. *Geophysics*, **59**(6):983-999.

Cohen J.K. & Stockwell J.W. 2010. *CWP/SU: Seismic Un*x Release No. 42: an open source software package for seismic research and processing*. Center for Wave Phenomena, Colorado School of Mines.

Dix C.H. 1955. Seismic velocities from surface measurements. *Geophysics*, **20**(1):68-86.

Fomel S. 2004. On anelliptic approximations for qP velocities in VTI media. *Geophysical Prospecting*, **52**(3):247-259.

Gazdag J. 1978. Wave-equation migration by phase-shift method. *Geophysics*, **43**:1342-1351.

Gazdag J. & Squazzero P. 1984. Migration of seismic data by phase shift plus interpolation. *Geophysics*, **49**(2):124-131.

Helbig K. 1994. *Foundation of Anisotropy for Exploration Seismics*. Pergamon, Oxford.

Malovichko A.A. 1978. A new representation of the traveltime curve of reflected waves in horizontally layered media. *Applied Geophysics*, **91**:47-53.

Stockwell Junior J.W. 1997. Free software in education: A case study of CWP/SU: Seismic Un*x. *The Leading Edge*, **16**(7):1045-1049.

Thomsen L. 1986. Weak elastic anisotropy. *Geophysics*, **51**(10):1954-1966.

Tsvankin I. & Thomsen L. 1994. Nonhyperbolic reflection moveout in anisotropic media. *Geophysics*, **59**(8):1290-1304.

Ursin B. & Stovas A. 2006. Traveltime approximations for a layered transversely isotropic medium. *Geophysics*, **71**(2):D23-D33.

Yilmaz O. 1987. *Seismic Data Processing*. Society of Exploration Geophysicists, Tulsa, Oklahoma.